Signalling pathway of nitric oxide in synaptic GABA release in the rat paraventricular nucleus

De-Pei Li, Shao-Rui Chen, Thomas F. Finnegan and Hui-Lin Pan

Department of Anaesthesiology, The Pennsylvania State University College of Medicine, The Milton S. Hershey Medical Center, Hershey, PA 17033, USA

In the paraventricular nucleus (PVN) of the hypothalamus, nitric oxide (NO) inhibits sympathetic outflow through increased GABA release. However, the signal transduction pathways involved in its action remain unclear. In the present study, we determined the role of cGMP, soluble guanylyl cyclase, and protein kinase G in the potentiating effect of NO on synaptic GABA release to spinally projecting PVN neurones. The PVN neurones were retrogradely labelled by a fluorescent tracer injected into the thoracic spinal cord of rats. Whole-cell voltage-clamp recordings were performed on labelled PVN neurones in the hypothalamic slice. Bath application of the NO donor, *S*-nitroso-*N*-acetyl-penicillamine (SNAP), reproducibly increased the frequency of miniature GABAergic inhibitory postsynaptic currents (mIPSCs) without changing the amplitude and the decay time constant. Neither replacement of Ca^{2+} with Co^{2+} nor application of Cd^{2+} to block the Ca^{2+} channel altered the effect of SNAP on mIPSCs. Also, the effect of SNAP on mIPSCs was not significantly affected by thapsigargin, a Ca^{2+}-ATPase inhibitor that depletes intracellular Ca^{2+} stores. Application of a membrane-permeant cGMP analogue, pCPT–cGMP, mimicked the effect of SNAP on mIPSCs in the presence of a phosphodiesterase inhibitor, IBMX. Furthermore, both the soluble guanylyl cyclase inhibitor, ODQ, and the specific protein kinase G inhibitor, Rp pCPT cGMP, abolished the effect of SNAP on mIPSCs. Thus, these data provide substantial new information that NO potentiates GABAergic synaptic inputs to spinally projecting PVN neurones through a cGMP–protein kinase G pathway.

(Received 14 August 2003; accepted after revision 10 October 2003; first published online 10 October 2003)
Corresponding author H.-L. Pan: Department of Anaesthesiology, The Pennsylvania State University College of Medicine, The Milton S. Hershey Medical Center, Hershey, PA 17033, USA. Email: hpan@psu.edu

The hypothalamic paraventricular nucleus (PVN) is a critical site for neuroendocrine control and homeostasis (Swanson & Sawchenko, 1983; de Wardener, 2001). The PVN contains many different output neurones including those projecting to the brainstem and the intermediolateral cell column of the spinal cord. These projection neurones are important in regulation of sympathetic outflow and cardiovascular function during physiological and pathophysiological conditions such as stress, hypertension, and congestive heart failure (Imaki *et al.* 1998; Allen, 2002; Zhang *et al.* 2002). In the PVN, nitric oxide (NO) regulates neuroendocrine and sympathetic vasomotor tone through alteration of GABA release and neuronal excitability (Zhang & Patel, 1998; Krukoff, 1999; Li *et al.* 2002). We have shown that NO suppresses the firing activity of spinally projecting PVN neurones through potentiation of GABAergic synaptic inputs (Li *et al.* 2002). However, the signalling mechanisms involved in the stimulatory effect of NO on presynaptic GABA release in the PVN are not clear.

As a membrane-permeant neuronal messenger in the central nervous system, NO produces its biological actions through distinct signal transduction pathways (Stamler *et al.* 1997; Ahern *et al.* 2002). Besides the modification of proteins involved in its action through *S*-nitrosylation (Jaffrey *et al.* 2001) or formation of peroxynitrite (Stamler *et al.* 1992; Trabace & Kendrick, 2000), NO initiates a signalling cascade by activating the soluble isoform of guanylyl cyclase (sGC) and subsequently elevates intracellular concentration of 3′,5′-cyclic guanosine monophosphate (cGMP) (Matsuoka *et al.* 1992; Southam & Garthwaite, 1993; Wood & Garthwaite, 1994). The principal targets of cGMP are cGMP-gated channels (Zagotta & Siegelbaum, 1996), cGMP-dependent phosphodiesterases (Pineda *et al.* 1996; Kraus & Prast, 2002), and cGMP-stimulated protein kinase G (PKG) (Jaffrey & Snyder, 1995). The NO–cGMP–PKG signalling pathway may be important in regulation of neuronal excitability and neurotransmission at pre- and postsynaptic sites. In this regard, L-arginine and sodium

 DOI: 10.1113/jphysiol.2003.053371

nitroprusside can increase neuronal excitability and dye coupling of supraoptic nucleus neurones through cGMP-dependent mechanisms in rats (Yang & Hatton, 1999). Also, a NO donor, *S*-nitroso-*N*-acetyl-penicillamine (SNAP), and a cGMP analogue, 8-Br-cGMP, increase the firing activity of neurones in the locus coeruleus (Pineda *et al.* 1996). *In vivo* microdialysis studies have shown that SNAP or 8-Br-cGMP increases the release of acetylcholine, glutamate, and GABA in the striatum (Guevara-Guzman *et al.* 1994; Trabace & Kendrick, 2000). Furthermore, the cGMP analogue pCPT-cGMP facilitates glutamate release in the nerve terminals (Klyachko *et al.* 2001). The PVN is not only rich in neuronal NO synthase (nNOS) but also in both the α1 and β1 subunits of sGC (Furuyama *et al.* 1993; Li *et al.* 2002). However, the functional role of cGMP and sGC in NO-induced synaptic GABA release in the PVN has not been determined previously.

Neurotransmitter release from the nerve terminals is generally thought to be mediated by a Ca^{2+}-dependent mechanism. However, the effect of NO on the synaptic neurotransmitter release appears to be an exception. In this regard, NO can stimulate Ca^{2+}-independent glutamate release from hippocampal synaptosomes (Meffert *et al.* 1994). Also, 8-Br-cGMP has little effect on both resting potential- and action potential-dependent increments of Ca^{2+} concentration in presynaptic terminal although it can potentate neurotransmitter release (Yawo, 1999). It has been suggested that NO-stimulated vesicle release is probably mediated through modulating synaptic vesicle docking and fusion reactions (Meffert *et al.* 1996). In the CNS, the effect of NO on neurotransmitter release is site specific with regard to the type of neurone and neurotransmitter. It has been shown that the effect of NO appears to be cell-type specific in the hypothalamus (Yang & Hatton, 1999; Ozaki *et al.* 2000; Li *et al.* 2002). In the present study, we used a combination of retrograde tracing and *in vitro* whole-cell recordings to determine the signal transduction mechanisms involved in NO-induced presynaptic GABA release to spinally projecting PVN neurones.

Methods

Retrograde labelling of spinally projecting PVN neurones

Sprague-Dawley rats (4–6 weeks old; Harlan, Indianapolis, IN, USA) of either sex were used for this study. The surgical preparations and experimental protocols were approved by the Animal Care and Use Committee of the Pennsylvania State University College of Medicine and conformed to the NIH guidelines on the ethical use of animals. All efforts were made to minimize both the suffering and number of animals used. The rat spinal cord at the T1–T4 level was exposed through dorsal laminectomy under halothane anaesthesia. A rhodamine-labelled fluorescent microsphere suspension (FluoSpheres, 0.04 μm, Molecular Probes, Eugene, OR, USA) was pressure-ejected (Picospritzer II, General Valve Co., Fairfield, NJ, USA) bilaterally into the region of the intermediolateral cell column of the spinal cord in 2 or 3 separate 50 nl injections using a glass micropipette (20–30 μm tip diameter). The pipette was positioned with a micromanipulator at about 500 μm below the dorsolateral sulcus, and the injection of FluoSpheres was monitored through a surgical microscope (Li *et al.* 2002, 2003). After injection, the muscle and skin were sutured and the wound was closed. Animals were returned to their cages for 3–7 days, which is sufficient time to permit retrograde tracer to be transported to the PVN.

Slice preparations

A total of 46 rats were used for the electrophysiology experiments. Three to seven days after FluoSpheres injection, the rats were rapidly decapitated under halothane anaesthesia. The brain was quickly removed and placed in ice-cold artificial cerebral spinal fluid (aCSF) perfusion solution saturated with 95% O_2 and 5% CO_2 for 1–2 min. A tissue block containing the hypothalamus was cut from the brain and glued on to the stage of the vibratome (Technical Product International, St Louis, MO, USA), as we previously described (Li *et al.* 2002, 2003). Coronal slices (300 μm in thickness) containing the PVN were cut from the tissue block in ice-cold aCSF. The slices were preincubated in the aCSF, which was saturated and continuously gassed with 95% O_2 and 5% CO_2 at 34°C for 1 h until they were transferred to the recording chamber. The perfusion solution contained (mM): 124.0 NaCl, 3.0 KCl, 1.3 $MgSO_4$, 2.4 $CaCl_2$, 1.4 NaH_2PO_4, 10.0 glucose, and 26.0 $NaHCO_3$. For the Ca^{2+}-free solution, Ca^{2+} was replaced with an equimolar concentration of Co^{2+} in the perfusion solution.

Recordings of postsynaptic currents of labelled PVN neurones

Recordings of miniature postsynaptic currents were performed in a radio frequency-shielded room using the whole-cell voltage-clamp technique, as we previously described (Li *et al.* 2002, 2003). The recording pipettes were triple-pulled from borosilicate capillaries (1.2 mm o.d., 0.68 mm i.d.; World Precision Instruments, Sarasota, FL, USA) using a micropipette puller (P-97, Sutter

Instrument, Novato, CA, USA). The resistance of the pipette was 3–5 MΩ when it was filled with a solution containing (mM): KCl, 140.0; $MgCl_2$, 1.0; Hepes, 10.0; EGTA, 10.0; $CaCl_2$, 1.0; and ATP-Mg, 2.0; adjusted to pH 7.25 with 1 M KOH (270–300 mosmol l^{-1}). The slice was placed in a glass-bottomed recording chamber (Warner Instruments, Hamden, CT, USA) and fixed with a grid of parallel nylon threads supported by a U-shaped stainless steel weight. The slice was perfused at 3.0 ml min^{-1} at 34°C maintained by an in-line solution heater and a temperature controller (model TC-324, Warner Instruments). It took ∼1.5 min to completely exchange the solution inside the recording chamber at the perfusion speed of 3.0 ml min^{-1}. Whole-cell recordings from labelled PVN neurones were made under visual control using a combination of epifluoresence illumination and infrared and differential interference contrast optics on an upright microscope (BX50WI, Olympus, Japan). The labelled neurones located in the medial third of the PVN area between the third ventricle and the fornix were selected for recording. The labelled PVN neurones were briefly identified with the aid of epifluorescence illumination. The identified cell was then visualized through a camera and a video monitor using infrared and differential interference contrast optics (Fig. 1*A* and *B*). A tight giga-ohm seal was obtained by application of slight negative pressure and the cell membrane was then ruptured by further suction. Recordings of postsynaptic currents began 5 min later after the whole-cell access was established and the current reached a steady state. The input resistance was monitored, and the recording was abandoned if it changed more than 15%. Recordings were performed with an Axopatch 200B amplifier (Axon Instruments, Union City, CA, USA). Signals were filtered at 1–2 kHz, digitized at 10 kHz using Digidata 1320 A (Axon Instruments), and saved to the hard drive of a computer. At a holding potential of –70 mV and in the presence of tetrodotoxin (TTX, 1 μM) and CNQX (6-cyano-7-nitroquinoxaline-2,3-dione, 20 μM), only miniature GABAergic inhibitory postsynaptic currents (mIPSCs) are recorded in the PVN (Li *et al.* 2002, 2003). The miniature excitatory postsynaptic currents (mEPSCs) were recorded in the presence of TTX (1 μM) and bicuculline (20 μM).

Drugs were applied to the recording chamber at final concentrations. SNAP, ODQ (1H-[1,2,4]oxadiazolo[4,3-a]quinoxalin-1-one), pCPT–cGMP (8-(4-chlorophenylthio)-guanosine 3′,5′-cylic monophosphate), Rp-pCPT-cGMP (Rp-8-[(4-chlorophenyl)thio]-cGMPS), IBMX (3-iso-butyl-1-methylxanthine), CNQX, and bicuculline methiodide were obtained from Sigma (St Louis, MO, USA). Fluorescence FluoSpheres were bought from Molecular Probes (Eugene, OR, USA). TTX was purchased from Alomone Laboratories (Jerusalem, Israel). All the drugs were prepared immediately before the experiments and applied to the recording chamber using syringe pumps.

Data analysis

Data are presented as means ± S.E.M. The mIPSCs and mEPSCs were analysed off-line with a peak detection program (MiniAnalysis, Synaptosoft Inc., Leonia, NJ, USA). Measurement of the amplitude and frequency and the decaying time constant of postsynaptic currents were performed for a period of 3 min during the control and drug application. The mIPSCs and mEPSCs were detected by the fast rise time of the signal over a threshold amplitude set at 6–10 pA above the background noise (Li *et al.* 2002, 2003). The cumulative probability of the amplitude and interevent interval of mEPSCs/mIPSCs was compared

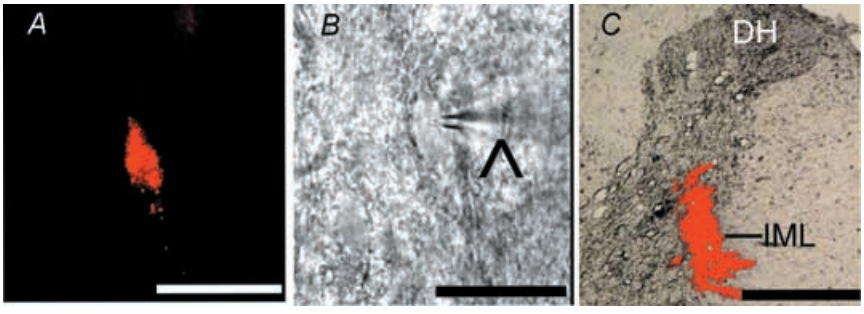

Figure 1. identification of retrogradely labeled spinally projecting PVN neurons
A, a PVN neurone in the brain slice labelled with FluoSphere identified with fluorescence illumination. *B*, the same neurone recorded with a glass electrode (^) viewed with Nomarski optics. *C*, photomicrograph showing the FluoSphere injection site (red) at the spinal intermediolateral cell column (IML) in one rat. Note that the bright field and fluorescence images were taken from the same tissue section and superimposed to show the location and diffusion of the FluoSphere injection. Scale bar, 50 μM in *A* and *B*; 500 μM in *C*. DH, dorsal horn.

using the Kolmogorov-Smirnov test, which estimates the probability that two cumulative distributions are similar. At least 100 randomly selected mIPSCs and mEPSCs were used in each analysis. All the decay phases of mIPSCs were analysed with one and two exponential functions. Based on the curve fitting R^2 values, all mIPSCs were best fitted by two components under all conditions. The effects of drugs on the amplitude and frequency of mIPSCs and mEPSCs were determined by the non-parametric Wilcoxon signed rank test or non-parametric ANOVA (Kruskal-Wallis) with Dunn's *post hoc* test. $P < 0.05$ was considered to be statistically significant.

Results

Whole-cell voltage-clamp recordings were obtained from a total of 68 FluoSphere-labelled PVN cells ($n = 46$ rats). To verify the injection and diffusion site of FluoSpheres in the thoracic spinal cord, the spinal cord was taken out after killing the animal and sectioned at the injection level. The spinal cord slices were then viewed under a microscope equipped with fluorescence illumination. The injection site of FluoSpheres was located in and around the intermediolateral cell column of the spinal cord, and the diffusion size of FluoSphere around the site of injection was about 0.5 mm in diameter (Fig. 1*C*). The labelled PVN neurones displayed a resting membrane potential of −61.6 ± 1.1 mV and an input resistance of 489.6 ± 28.3 MΩ.

Effect of SNAP on GABAergic mIPSCs of labelled PVN neurones

To test the effect of NO on spontaneous mIPSCs in labelled PVN neurones, an NO donor, SNAP, was used. The spontaneous mIPSCs recorded from the labelled neurones were completely abolished by bath application of 20 μM bicuculline ($n = 9$), the antagonist of $GABA_A$ receptors

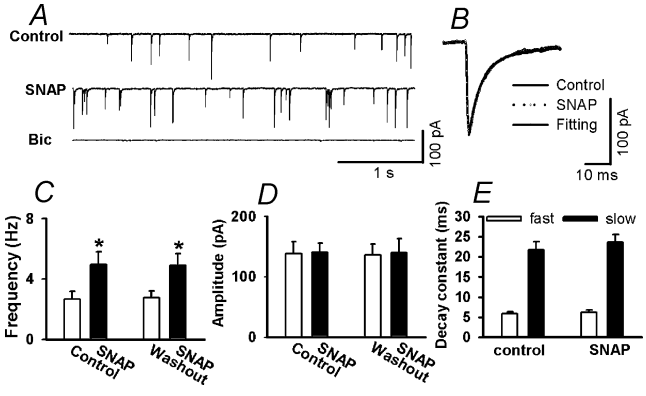

Figure 2. Effect of SNAP on GABAergic mIPSCs of labeled PVN neurons

A, representative tracings showing mIPSCs recorded from a labelled PVN neurone during control, application of 100 μM SNAP, and application of 20 μM bicuculline. Note that bicuculline completely abolished mIPSCs. *B*, superimposed averages of 100 consecutive mIPSCs obtained during control and SNAP application. The decay time constants during control ($\tau_{fast} = 4.83$ ms and $\tau_{slow} = 25.75$ ms) and SNAP administration ($\tau_{fast} = 4.86$ ms and $\tau_{slow} = 25.89$ ms) were similar. *C* and *D*, summary data showing the effect of 100 μM SNAP on the frequency (*C*) and the amplitude (*D*) of mIPSCs of nine labelled PVN neurones. *E*, summary data showing the decay time constants of mIPSCs of nine labelled PVN neurones during control and administration of 100 μM SNAP. Data presented as means ± S.E.M. * $P < 0.05$ compared to the control (Kruskal-Wallis test). Bic, bicuculline.

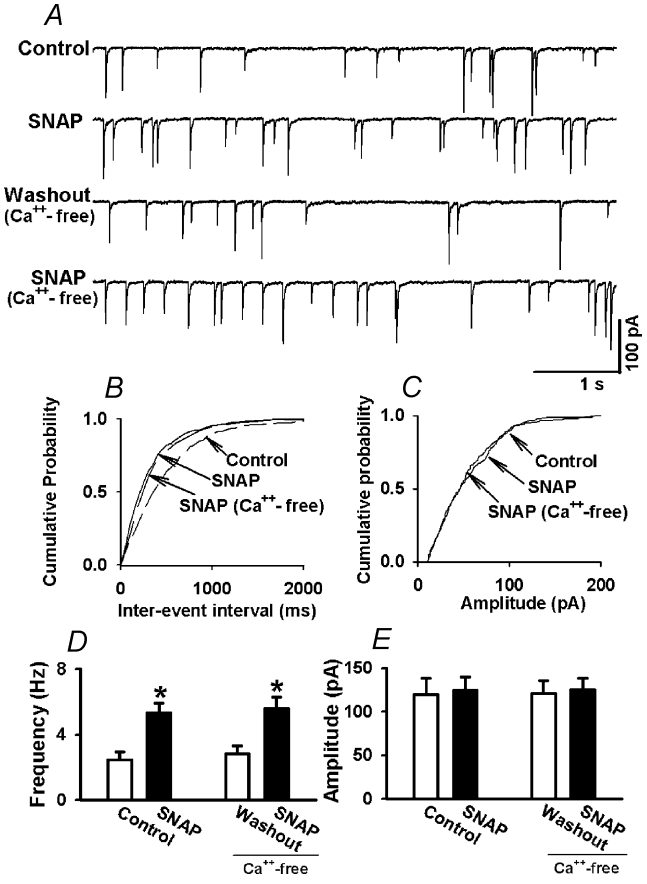

Figure 3. Effect of SNAP on mIPSCs of labeled PVN neurons in Ca^{2+}-free solution

A, representative tracings showing the effect of 100 μM SNAP on mIPSCs in normal aCSF and Ca^{2+}-free aCSF. *B* and *C*, cumulative plot analysis of mIPSCs of the same neurone as in *A* showing the distribution of the interevent interval (*B*) and peak amplitude (*C*) during control, application of 100 μM SNAP, and SNAP application in Ca^{2+}-free aCSF. SNAP decreased the interevent interval of mIPSCs ($P < 0.05$, Kolmogorov-Smirnov test) without changing the distribution of the amplitude in both normal and Ca^{2+}-free aCSF.
D and *E*, summary data showing the effect of SNAP on the frequency (*D*) and the amplitude (*E*) of mIPSCs of eight labelled PVN neurones in both normal and Ca^{2+}-free aCSF. Data presented as means ± S.E.M. * $P < 0.05$ compared to the control (Kruskal-Wallis test).

(Fig. 2*A*). SNAP, at a concentration of 100 μM, significantly increased the frequency of mIPSCs from 2.67 ± 0.52 to 4.98 ± 0.64 Hz without affecting the kinetics and amplitude of mIPSCs (138.6 ± 19.4 *versus* 140.5 ± 15.2 pA) (Fig. 2*B*, *C* and *D*). Neither the fast (5.89 ± 0.42 *versus* 6.20 ± 0.55 ms) nor slow (21.67 ± 2.02 *versus* 23.59 ± 1.98 ms) component of the decay phase of mIPSCs during SNAP application was significantly different from those during the control ($n = 9$, Fig. 2*E*). Repeat application of SNAP had a reproducible excitatory effect on the frequency of mIPSCs (Fig. 2*C*). In four separate labelled PVN neurones, 100 μM SNAP had no significant effect on the peak amplitude of electrically evoked IPSCs (300 ± 57 *versus* 306 ± 58 pA, $P > 0.05$).

Role of Ca^{2+} and Ca^{2+} channels in the effect of SNAP on mIPSCs

To examine whether the SNAP-induced increase in the frequency of mIPSCs was dependent on extracellular Ca^{2+}, the effect of SNAP on mIPSCs was tested in a Ca^{2+}-free aCSF. In this experiment, Ca^{2+} was removed and replaced by an equimolar concentration of Co^{2+} in the perfusion solution. In eight labelled PVN cells, following testing the initial effect of SNAP (100 μM) on mIPSCs, the perfusion solution was replaced by the Ca^{2+}-free aCSF. The frequency and the amplitude of mIPSCs was not affected by perfusion of the Ca^{2+}-free aCSF (Fig. 3). Subsequent application of SNAP (100 μM) still significantly increased the frequency of mIPSCs in the Ca^{2+}-free aCSF (from 2.8 ± 0.5 to 5.5 ± 0.7 Hz, $P < 0.05$) without affecting the amplitude of mIPSCs in these eight neurones (Fig. 3).

To further determine the role of Ca^{2+} channels in SNAP-induced increase in mIPSCs, the non-specific calcium channel blocker, Cd^{2+}, was also used in another nine labelled PVN neurones. After examining the initial effect of bath application of 100 μM SNAP on mIPSCs, Cd^{2+} (50–100 μM) was added to the slice recording chamber. Cd^{2+} alone had no significant effect on the frequency and amplitude of mIPSCs of labelled PVN neurones. Application of SNAP (100 μM) still increased significantly the frequency of mIPSCs in the presence of Cd^{2+} (from 3.1 ± 0.5 to 5.9 ± 0.6 Hz, $P < 0.05$) without changing the amplitude and the decay time constant of mIPSCs (Fig. 4).

It has been shown that NO can increase the mitochondrial calcium release in neurones (Horn *et al.* 2002). To determine if the effect of NO on mIPSCs

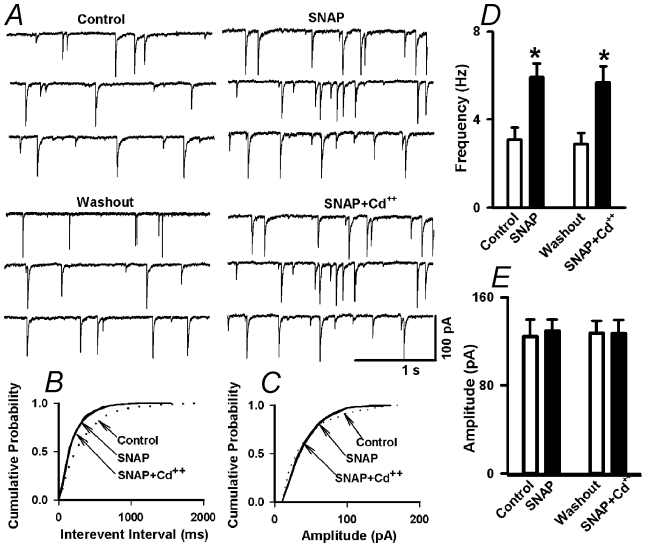

Figure 4. Effect of SNAP on mIPSCs after blockade of Ca^{2+} channels with Cd^{2+}

A, raw tracings showing the effect of 100 μM SNAP and SNAP + 50 μM Cd^{2+} on mIPSCs of a labelled PVN neurone. Note that treatment with Cd^{2+} failed to alter the SNAP-induced increase in the frequency of mIPSCs. *B* and *C*, cumulative probability analysis of mIPSCs of the same neurone as in *A* showing the distribution of the interevent interval (*B*) and peak amplitude (*C*) during control, SNAP, and application of SNAP + Cd^{2+}. SNAP decreased the interevent interval of mIPSCs ($P < 0.05$, Kolmogorov-Smirnov test) without changing the distribution of the amplitude in the presence of Cd^{2+}. *D* and *E*, summary data showing the effect of SNAP and SNAP + Cd^{2+} on the frequency (*D*) and amplitude (*E*) of mIPSCs of nine labelled PVN neurones. $^*P < 0.05$ compared to the control (Kruskal-Wallis test).

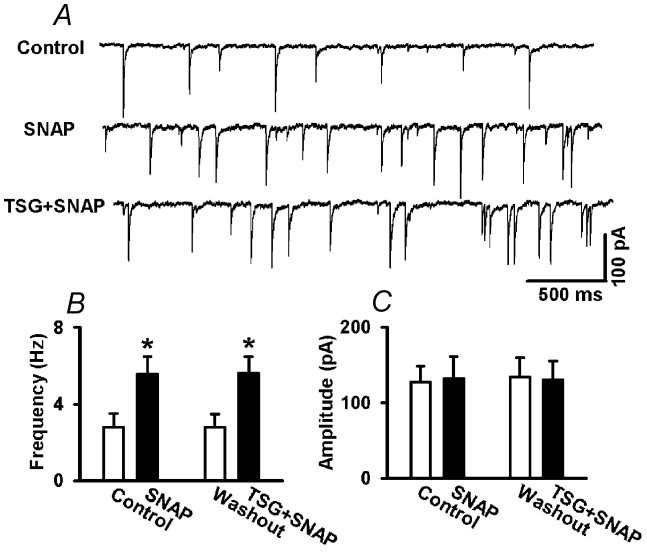

Figure 5. Role of introcellular Ca^{2+} store in the effect of SNAP on mIPSCs

A, Original tracings showing mIPSCs recorded from a labelled PVN neurone during control, application of 100 μM SNAP, and application of SNAP in the presence of 10 μM thapsigargin (TSG). *B* and *C*, summary data showing the effect of 100 μM SNAP on the frequency (*B*) and the amplitude (*C*) of mIPSCs before and after treatment with 10 μM thapsigargin in six labelled PVN neurones. Data presented as means ± S.E.M. $^*P < 0.05$ compared to the control (Kruskal-Wallis test).

is caused by Ca^{2+} release from the intracellular store, we examined the effect of 100 μM SNAP on mIPSCs before and after treatment with 10 μM thapsigargin, a Ca^{2+}-ATPase inhibitor that depletes intracellular Ca^{2+} stores (Tanabe *et al.* 1998). Application of thapsigargin produced an initial increase in the frequency of mIPSCs (from 2.78 ± 0.72–4.87 ± 0.94 Hz, $P < 0.05$) but not the amplitude of mIPSCs (126.8 ± 21.35 *versus* 132.5 ± 27.68 pA), and such an effect only lasted 3–5 min. Following treatment with thapsigargin, 100 μM SNAP similarly increased the frequency but not the amplitude of mIPSCS in all six labelled PVN neurones (Fig. 5).

Effect of cGMP analogue on mIPSCs and mEPSCs

To investigate the role of cGMP in the effect of NO on synaptic GABA release to labelled PVN neurones, we tested the effect of pCPT-cGMP, a membrane-permeable analogue of cGMP, on mIPSCs. To minimize the hydrolysis of cGMP and the cGMP analogue in nerve terminals, the effect of pCPT-cGMP was examined in the presence of an inhibitor of phosphodiesterases, IBMX (100 μM) (Yawo, 1999). In the pilot experiment, pCPT-cGMP produced an inconsistent effect on mIPSCs in six cells examined in the absence of IBMX (data not shown). In the presence of 100 μM IBMX, application of 30 μM pCPT-cGMP consistently increased the frequency of mIPSCs from 2.36 ± 0.45–4.98 ± 0.56 Hz ($P < 0.05$) without affecting the amplitude and the decay time constant of mIPSCs in all nine neurones tested (Fig. 6). IBMX (100 μM) alone

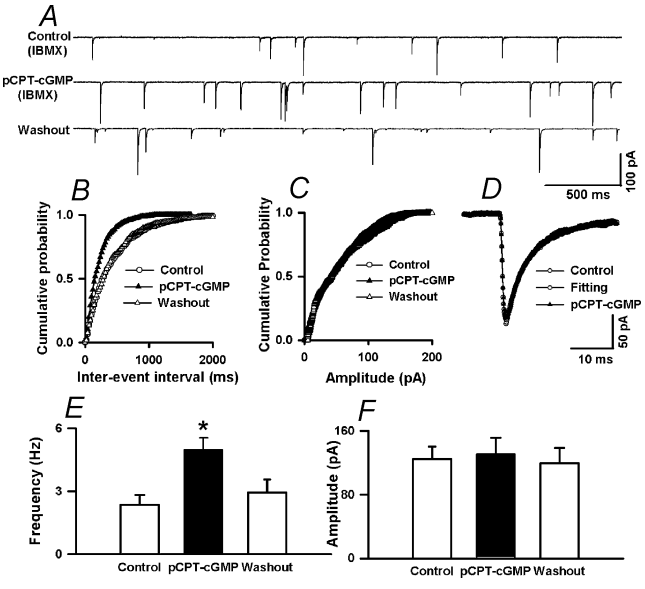

Figure 6. Lack of effect of pCPT-cGMP on mEPSCs in labeled PVN neurons
A, raw tracings showing the spontaneous mIPSCs during control and application of 30 μM pCPT–cGMP in the presence of 100 μM IBMX in a labelled PVN neurone. *B* and *C*, cumulative plot analysis of mIPSCs of the same neurone as in *A* showing the distribution of the interevent interval (*B*) and peak amplitude (*C*) during control and pCPT–cGMP application in the presence of IBMX. pCPT–cGMP decreased the interevent interval of mIPSCs (Kolmgorov-Smirnov test, $P < 0.05$) without changing the distribution of the amplitude. *D*, superimposed averages of 100 consecutive mIPSCs obtained during control and pCPT–cGMP application. The decay time constants during control ($\tau_{fast} = 4.79$ ms and $\tau_{slow} = 23.12$ ms) and pCPT–cGMP administration ($\tau_{fast} = 4.74$ ms and $\tau_{slow} = 22.25$ ms) were similar. *E*,*F*, summary data showing the effect of pCPT–cGMP on the frequency (*E*) and amplitude (*F*) of mIPSCs of nine labelled PVN neurones. Data presented as means ± S.E.M. $^*P < 0.05$ compared to the control (Kruskal-Wallis test).

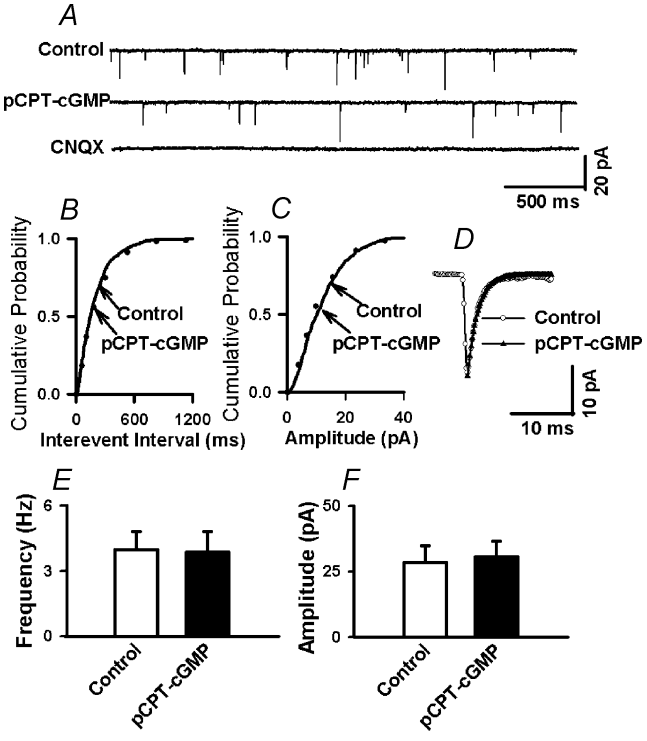

Figure 7. pCPT-cGMP potentiates mIPSCs in labeled PVN neurons
A, representative tracings from a PVN-labelled neurone showing mEPSCs during control, application of 50 μM pCPT–cGMP, and application of 20 μM CNQX in the presence of 100 μM IBMX. Note that CNQX completely eliminated mEPSCs. *B* and *C*, cumulative plot analysis of mEPSCs of the same neurone as in *A* showing the distribution of the interevent interval (*B*) and peak amplitude (*C*) during control and pCPT–cGMP application. Neither the frequency nor the amplitude of mEPSCs was altered by the pCPT–cGMP. *D*, superimposed averages of 100 consecutive mEPSCs obtained during control and pCPT–cGMP application. The decay phase of mEPSCs was best fitted with a single exponential function. The decay time constant was similar during control ($\tau = 1.77$ ms) and pCPT–cGMP application ($\tau = 1.74$ ms). *E*, *F*, summary data showing the effect of 50 μM pCPT–cGMP on the frequency (*E*) and amplitude (*F*) of mEPSCs in eight labelled PVN neurones. Data presented as means ± S.E.M. (Wilcoxon Signed rank test).

had no significant effect on the frequency and amplitude of mIPSCs (2.32 ± 0.41 to 2.38 ± 0.46 Hz, $P > 0.05$). The cumulative probability analysis of mIPSCs before and during pCPT-cGMP application revealed that the distribution pattern of the interevent interval of mIPSCs shifted toward the left in response to pCPT-cGMP, while the distribution pattern of the amplitude of mIPSC was not significantly changed (Fig 6*B* and *C*). The effect of pCPT-cGMP on mIPSCs was further analysed by measuring the time constant of the decay phase of spontaneous mIPSCs. Neither the fast (4.96 ± 0.39 *versus* 5.02 ± 0.25 ms) nor slow (18.63 ± 2.43 *versus* 19.45 ± 2.39 ms) component of the decay phase of mIPSCs during pCPT-cGMP application was significantly different from those during the control (Fig. 6*D*).

We have shown that SNAP selectively increases the frequency of mIPSCs without affecting mEPSCs (Li *et al.* 2002). To evaluate whether pCPT-cGMP has an effect that is similar to that of SNAP, the effect of pCPT-cGMP on mEPSCs was tested in the presence of 100 μM IBMX in another eight labelled PVN cells. The mEPSCs were eliminated by application of 20 μM CNQX (Fig. 7*A*). pCPT-cGMP (30 μM) had no significant effect on the frequency and amplitude of mEPSCs in these eight neurones in the presence of 100 μM IBMX (Fig. 7). Also,

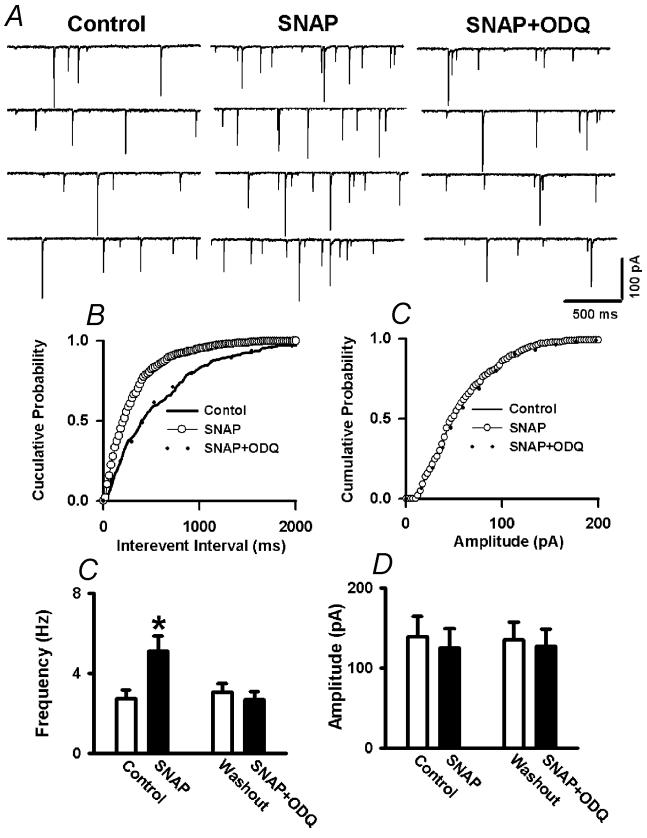

Figure 8. ODQ blocks the effect of SNAP on mIPSCs
A, representative tracings showing the spontaneous mIPSCs during control, perfusion of 100 μM SNAP and SNAP plus 30 μM ODQ in labelled PVN neurones. Note that treatment with ODQ abolished SNAP-induced increase in the frequency of mIPSCs. *B*,*C*, cumulative plot analysis of mIPSCs of the same neurone showing the distribution of the interevent interval (*B*) and peak amplitude (*C*) during control, application of SNAP, and application of SNAP + ODQ. *D*,*E*, summary data showing the effect of SNAP and SNAP + ODQ on the frequency (*D*) and amplitude (*E*) of mIPSCs in 11 labelled PVN neurones. Data presented as means ± S.E.M. $^*P < 0.05$ compared to control (Kruskal-Wallis test).

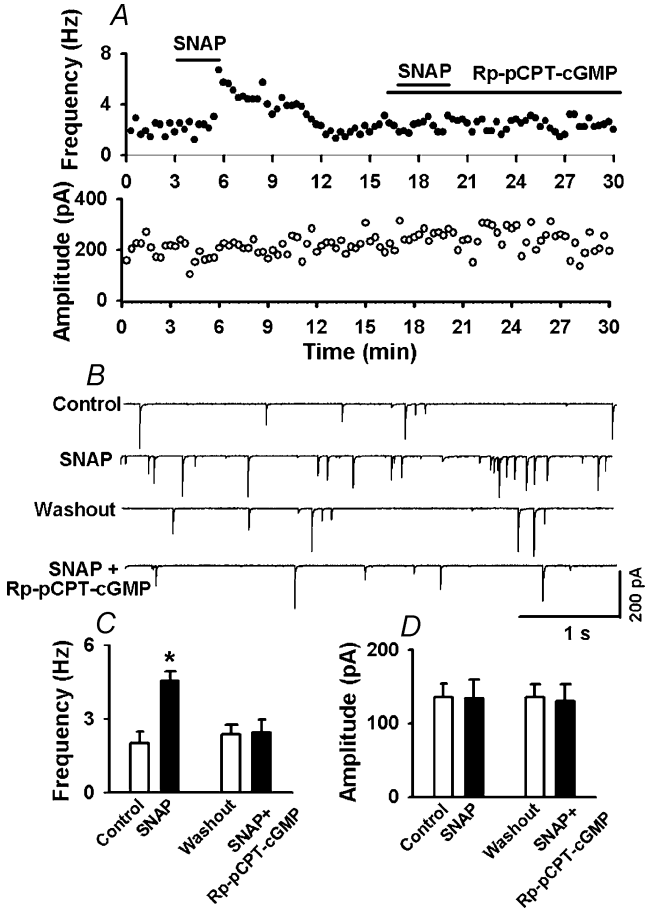

Figure 9. Rp-pCPT-cGMP inhibits the effect of SNAP on mIPSCs
A, histograms showing the effect of 100 μM SNAP and SNAP + 1 μM Rp-pCPT-cGMP on the frequency (upper panel) and amplitude (lower panel) of spontaneous mIPSCs in a labelled PVN neurone. *B*, representative tracings showing the spontaneous mIPSCs during control, application of SNAP, and SNAP + Rp-pCPT-cGMP in the same neurone as in *A*. Note that Rp-pCPT-cGMP completely abolished the SNAP-induced increase in the frequency of mIPSCs. *C* and *D*, summary data showing the effect of SNAP and SNAP + Rp-pCPT-cGMP on the frequency (*C*) and amplitude (*D*) of mIPSCs of nine labelled PVN neurones. Data presented as means ± S.E.M. $^*P < 0.05$ compared to control (Kruskal-Wallis test).

pCPT-cGMP had no effect on the frequency of mEPSCs even at a higher concentration (50 μM) (2.53 ± 0.81 *versus* 2.68 ± 0.93 Hz, $P > 0.05$). The effect of 50 μM pCPT-cGMP on mEPSCs was further analysed by measuring the time constant of the decay phase of mEPSCs. The decay time constant of mEPSCs was best fitted by a single exponential function (Fig. 7*D*). The decay time constant of mEPSCs was similar during control and pCPT-cGMP application (1.86 ± 0.13 *versus* 1.97 ± 0.19 ms, $P > 0.05$, $n = 8$).

Role of sGC in the effect of NO on mIPSCs

To determine whether the action of NO on mIPSCs is through activation of sGC, ODQ (10 μM), a selective inhibitor of the NO-activated sGC, was used in 11 labelled PVN neurones. Following testing the initial effect of 100 μM SNAP on mIPSCs, 10 μM ODQ was perfused into the recording chamber. In the presence of ODQ, SNAP failed to increase the frequency of mIPSCs (2.74 ± 0.75 *versus* 2.70 ± 0.41 Hz, $P > 0.05$, Fig. 8).

Role of PKG in the effect of NO on mIPSCs

To further determine if PKG is involved in the effect of SNAP on mIPSCs, the effect of Rp-pCPT-cGMP, a specific membrane-permeable PKG inhibitor, was tested in an additional nine labelled cells. SNAP initially increased the frequency of mIPSCs from 2.87 ± 0.45 to 5.84 ± 0.65 Hz ($P < 0.05$, Fig. 9). However, following treatment with 1 μM Rp-pCPT-cGMP, the excitatory effect of SNAP on mIPSCs was completely abolished (2.82 ± 0.51 *versus* 2.76 ± 0.49 Hz, $P > 0.05$, Fig. 9).

Discussion

This is the first study investigating the signal transduction pathways involved in the potentiating effect of NO on GABAergic synaptic inputs to spinally projecting PVN neurones. We found that neither replacement of Ca^{2+} with Co^{2+} nor blockade of the Ca^{2+} channel with Cd^{2+} altered the effect of SNAP on the increase in the frequency of GABAergic mIPSCs. Also, the effect of SNAP on mIPSCs was not significantly altered by thapsigargin, a Ca^{2+}-ATPase inhibitor that depletes intracellular Ca^{2+} stores. These data suggest that extracellular and intracellular Ca^{2+} and Ca^{2+} channels are not involved in the excitatory effect of SNAP on synaptic GABA release in the PVN. A membrane permeant cGMP analogue, pCPT-cGMP, mimicked the excitatory effect of SNAP on the frequency of mIPSCs, but had no effect on glutamatergic mEPSCs. Furthermore, the effect of SNAP on mIPSCs was eliminated by application of an inhibitor of sGC, ODQ, and a specific PKG inhibitor, Rp-pCPT-cGMP. Thus, the present study provides substantial new evidence that NO increases presynaptic GABA release to spinally projecting PVN neurones through a cGMP–PKG-dependent mechanism.

The PVN is a heterogenous region containing interneurones and many output neurones projecting to the posterior pituitary, rostral ventrolateral medulla, nucleus of the solitary tract, and intermediolateral cell column of the spinal cord (Swanson & Sawchenko, 1983; Shafton *et al.* 1998). Hyperactivity of PVN neurones plays an important part in the maintenance of increased sympathetic vasomotor tone in certain types of hypertension (Herzig *et al.* 1991; Takeda *et al.* 1991; Allen, 2002). Decreased GABAergic inhibition of presympathetic neurones in the PVN may be responsible for the elevated level of sympathetic outflow in hypertension (de Wardener, 2001). NO is an important inhibitory modulator in the PVN and may function as a 'physiological brake' to prevent over-excitation of PVN neurones and the sustained increase in sympathetic outflow (Zhang & Patel, 1998; Li *et al.* 2002). We have shown that NO inhibits the excitability of spinally projecting PVN neurones through potentiation of GABAergic synaptic inputs (Li *et al.* 2002). However, the signalling mechanisms responsible for NO-induced augmentation of GABA release to spinally projecting PVN neurones are not known. In the present study, the PVN neurones projecting to the spinal cord were identified using the retrograde labelling technique in order to specifically study this population of neurones related to the control of sympathetic efferent activity.

The neurotransmitter release from the presynaptic terminals is usually mediated through a Ca^{2+}-dependent mechanism. It has been shown that NO-induced GABA release from cerebrocortical neurones is dependent on Ca^{2+} influx (Ohkuma *et al.* 1998). However, NO does not increase intracellular Ca^{2+} in cultured hippocampal neurones (Sporns & Jenkinson, 1997). Also, NO can stimulate synaptic glutamate release in the hippocampal synaptosomes, independent of Ca^{2+} (Meffert *et al.* 1994, 1996). Furthermore, a decreased presynaptic intracellular Ca^{2+} following exposure to NO has been reported, and the Ca^{2+} channel blocker, Cd^{2+}, has no effect on NO-stimulated release of glutamate from hippocampal synaptosomes (Meffert *et al.* 1994). In the present study, we found that neither replacement of extracellular Ca^{2+} with Co^{2+} nor administration of Cd^{2+}, the voltage-dependent Ca^{2+} channel blocker, altered the NO-induced increase in the frequency of GABAergic mIPSCs of PVN–spinal neurones. Additionally, although NO can

increase the mitochondrial calcium release in neurones, its effect is not mediated by cGMP (Horn *et al.* 2002). In this study, we found that the effect of SNAP was persistent following treatment with thapsigargin, a Ca^{2+}-ATPase inhibitor that depletes intracellular Ca^{2+} stores (Tanabe *et al.* 1998). Thus, these findings suggest that NO-induced increase in synaptic GABA release to spinally projecting PVN neurones is not dependent on extracellular and intracellular Ca^{2+} and voltage-dependent Ca^{2+} channels. We observed that SNAP had little effect on the peak amplitude of electrically evoked IPSCs. Unlike mIPSCs, electrically evoked IPSCs are calcium dependent (Cd^{2+} completely blocked evoked IPSCs, data not shown), which is different from the action of NO on spontaneous mIPSCs. Also, we have shown that NO has a general inhibitory effect on the action potential of PVN neurones (Li *et al.* 2002). Therefore, the observed effect of NO on synaptic GABA release to spinally projecting PVN neurones is unrelated to the action potential.

Although different mechanisms may be responsible for NO-mediated pre or postsynaptic modulation, the NO–cGMP pathways appear to be involved in the action of NO in the CNS (Stamler *et al.* 1997; Ahern *et al.* 2002). Previous studies have shown that NO–cGMP mechanisms are involved in the presynaptic modulation in the hippocampus and nucleus accumbens (Boulton *et al.* 1994; Kraus & Prast, 2002), but the role of cGMP in the effect of NO on synaptic neurotransmitter release remains controversial. In this regard, cGMP reduces fast glutamatergic synaptic transmission in the rat hippocampus (Boulton *et al.* 1994). The cGMP analogue, 8-Br-cGMP, also produces a decrease in GABA and glutamate release to magnocellular neurones in the supraoptic nucleus (Ozaki *et al.* 2000). On the other hand, several studies have shown that cGMP produces an excitatory effect on the neurotransmitters release. For example, NO and cGMP can facilitate glutamate and GABA release in the nucleus accumbens (Kraus & Prast, 2002). Also, NO enhances Ca^{2+}-activated K^+ channel activity by stimulating sGC and PKG, and subsequently generates a use-dependent enhancement of neurotransmitter release in posterior pituitary nerve terminals (Klyachko *et al.* 2001). In our study, the excitatory effect of SNAP on GABAergic mIPSCs was mimicked by a more specific membrane permeant cGMP analogue, pCPT-cGMP. However, the frequency and amplitude of glutamatergic mEPSCs were not altered by pCPT-cGMP, an effect similar to that of L-arginine and SNAP (Li *et al.* 2002). Furthermore, we found that the specific sGC inhibitor, ODQ, completely abolished the SNAP-induced increase in the frequency of mIPSCs. These data suggest that NO-induced potentiation of GABAergic mIPSCs is mediated by cGMP in spinally projecting PVN neurones. sGC is considered as the receptor enzyme of NO, and activation of sGC enhances the formation of cGMP (Schmidt *et al.* 1993). The electrophysiology data in this study strongly support the hypothesis that NO potentiates synaptic GABA release to the PVN neurones through activation of sGC and formation of cGMP in the presynaptic terminals.

There are at least three molecular targets that may mediate the action of cGMP. These include cGMP-gated ion channels (Zagotta & Siegelbaum, 1996), cGMP-dependent phosphodiesterases (Schmidt *et al.* 1993; Pineda *et al.* 1996; Kraus & Prast, 2002), and PKG (Jaffrey & Snyder, 1995). Ca^{2+} is the main current carrier of cGMP-gated channels (Kaupp & Seifert, 2002). In the present study, replacement of Ca^{2+} with Co^{2+} failed to attenuate NO-induced potentiation of presynaptic GABA release. Thus, cGMP-gated channels are unlikely to be involved in NO-induced GABA release in the PVN. Since pCPT-cGMP still increased the frequency of mIPSCs in the presence of a phosphodiesterase inhibitor, IBMX, this suggests that the phosphodiesterase is not involved directly in the effect of NO on synaptic GABA release to PVN neurones. In this study, IBMX was used to inhibit the phosphodiesterase, and hence to minimize the hydrolysis of pCPT-cGMP and raise the intracellular pCPT-cGMP level. The type II PKG is widely expressed on axon terminals and dendrites in the brain including the PVN (de Vente *et al.* 2001). In the present study, we found that the specific PKG inhibitor, Rp-pCPT-cGMP, completely eliminated SNAP-induced potentiation of mIPSCs. Therefore, these data suggest that the NO-induced increase in synaptic GABA release to PVN–spinal neurones is through PKG activation targeted by cGMP.

The potential PKG substrates involved in the action of NO on enhanced GABAergic synaptic release in the PVN are not clear. We are not aware that any vesicle protein phosphorylated by PKG is present only on GABAergic but not glutamatergic synaptic terminals. Interestingly, some studies have suggested that opioids also have a selective action on GABAergic but not glutamatergic synapses, and the voltage-gated A-type potassium channel located on the GABAergic terminals appears to be involved in the inhibitory effect of opioids on GABA release (Vaughan *et al.* 1997; Pan *et al.* 2002). It has been shown recently that stimulation of PKG inhibits the voltage-gated A-type potassium channel in neurones (Liu & Simon, 2003). However, further studies are needed to determine if the voltage-gated A-type potassium channel is the target of PKG in the PVN.

In summary, the present study provides important new information about the signalling mechanisms through which NO augments GABAergic synaptic inputs to PVN–spinal neurones. Our data suggest that NO increases synaptic GABA release to spinally projecting PVN neurones through cGMP and PKG-dependent, but Ca^{2+}-independent, mechanisms. This new information is important to our understanding of the signal transduction mechanisms involved in the CNS action of NO in regulation of sympathetic vasomotor tone during physiological and pathological conditions.

References

Ahern GP, Klyachko VA & Jackson MB (2002). cGMP and S-nitrosylation: two routes for modulation of neuronal excitability by. *Trends Neurosci* **25**, 510–517.

Allen AM (2002). Inhibition of the hypothalamic paraventricular nucleus in spontaneously hypertensive rats dramatically reduces sympathetic vasomotor tone. *Hypertension* **39**, 275–280.

Boulton CL, Irving AJ, Southam E, Potier B, Garthwaite J & Collingridge GL (1994). The nitric oxide–cyclic GMP pathway and synaptic depression in rat hippocampal slices. *Eur J Neurosci* **6**, 1528–1535.

Furuyama T, Inagaki S & Takagi H (1993). Localizations of alpha 1 and beta 1 subunits of soluble guanylate cyclase in the rat brain. *Brain Res Mol Brain Res* **20**, 335–344.

Guevara-Guzman R, Emson PC & Kendrick KM (1994). Modulation of *in vivo* striatal transmitter release by nitric oxide and cyclic GMP. *J Neurochem* **62**, 807–810.

Herzig TC, Buchholz RA & Haywood JR (1991). Effects of paraventricular nucleus lesions on chronic renal hypertension. *Am J Physiol* **261**, H860–867.

Horn TF, Wolf G, Duffy S, Weiss S, Keilhoff G & MacVicar BA (2002). Nitric oxide promotes intracellular calcium release from mitochondria in striatal neurons. *FASEB J* **16**, 1611–1622.

Imaki T, Naruse M, Harada S, Chikada N, Nakajima K, Yoshimoto T & Demura H (1998). Stress-induced changes of gene expression in the paraventricular nucleus are enhanced in spontaneously hypertensive rats. *J Neuroendocrinol* **10**, 635–643.

Jaffrey SR, Erdjument-Bromage H, Ferris CD, Tempst P & Snyder SH (2001). Protein S-nitrosylation: a physiological signal for neuronal nitric oxide. *Nat Cell Biol* **3**, 193–197.

Jaffrey SR & Snyder SH (1995). Nitric oxide: a neural messenger. *Annu Rev Cell Dev Biol* **11**, 417–440.

Kaupp UB & Seifert R (2002). Cyclic nucleotide-gated ion channels. *Physiol Rev* **82**, 769–824.

Klyachko VA, Ahern GP & Jackson MB (2001). cGMP-mediated facilitation in nerve terminals by enhancement of the spike afterhyperpolarization. *Neuron* **31**, 1015–1025.

Kraus MM & Prast H (2002). Involvement of nitric oxide, cyclic GMP and phosphodiesterase 5 in excitatory amino acid and GABA release in the nucleus accumbens evoked by activation of the hippocampal fimbria. *Neuroscience* **112**, 331–343.

Krukoff TL (1999). Central actions of nitric oxide in regulation of autonomic functions. *Brain Res Brain Res Rev* **30**, 52–65.

Li DP, Chen SR & Pan HL (2002). Nitric oxide inhibits spinally projecting paraventricular neurons through potentiation of presynaptic GABA release. *J Neurophysiol* **88**, 2664–2674.

Li DP, Chen SR & Pan HL (2003). Angiotensin II stimulates spinally projecting paraventricular neurons through presynaptic disinhibition. *J Neurosci* **23**, 5041–5049.

Liu L & Simon SA (2003). Modulation of IA currents by capsaicin in rat trigeminal ganglion neurons. *J Neurophysiol* **89**, 1387–1401.

Matsuoka I, Giuili G, Poyard M, Stengel D, Parma J, Guellaen G & Hanoune J (1992). Localization of adenylyl and guanylyl cyclase in rat brain by *in situ* hybridization: comparison with calmodulin mRNA distribution. *J Neurosci* **12**, 3350–3360.

Meffert MK, Calakos NC, Scheller RH & Schulman H (1996). Nitric oxide modulates synaptic vesicle docking fusion reactions. *Neuron* **16**, 1229–1236.

Meffert MK, Premack BA & Schulman H (1994). Nitric oxide stimulates Ca(2+) -independent synaptic vesicle release. *Neuron* **12**, 1235–1244.

Ohkuma S, Katsura M, Hibino Y, Hara A, Shirotani K, Ishikawa E & Kuriyama K (1998). Mechanisms for facilitation of nitric oxide-evoked [^{3}H]GABA release by removal of hydroxyl radical. *J Neurochem* **71**, 1501–1510.

Ozaki M, Shibuya I, Kabashima N, Isse T, Noguchi J, Ueta Y, Inoue Y, Shigematsu A & Yamashita H (2000). Preferential potentiation by nitric oxide of spontaneous inhibitory postsynaptic currents in rat supraoptic neurones. *J Neuroendocrinol* **12**, 273–281.

Pan YZ, Li DP, Chen SR & Pan HL (2002). Activation of delta-opioid receptors excites spinally projecting locus coeruleus neurons through inhibition of GABAergic inputs. *J Neurophysiol* **88**, 2675–2683.

Pineda J, Kogan JH & Aghajanian GK (1996). Nitric oxide and carbon monoxide activate locus coeruleus neurons through a cGMP-dependent protein kinase: involvement of a nonselective cationic channel. *J Neurosci* **16**, 1389–1399.

Schmidt HH, Lohmann SM & Walter U (1993). The nitric oxide and cGMP signal transduction system: regulation and mechanism of action. *Biochim Biophys Acta* **1178**, 153–175.

Shafton AD, Ryan A & Badoer E (1998). Neurons in the hypothalamic paraventricular nucleus send collaterals to the spinal cord and to the rostral ventrolateral medulla in the rat. *Brain Res* **801**, 239–243.

Southam E & Garthwaite J (1993). The nitric oxide-cyclic GMP signalling pathway in rat brain. *Neuropharmacology* **32**, 1267–1277.

Sporns O & Jenkinson S (1997). Potassium ion- and nitric oxide-induced exocytosis from populations of hippocampal synapses during synaptic maturation *in vitro*. *Neuroscience* **80**, 1057–1073.

Stamler JS, Singel DJ & Loscalzo J (1992). Biochemistry of nitric oxide and its redox-activated forms. *Science* **258**, 1898–1902.

Stamler JS, Toone EJ, Lipton SA & Sucher NJ (1997). (S) NO signals: translocation, regulation, and a consensus motif. *Neuron* **18**, 691–696.

Swanson LW & Sawchenko PE (1983). Hypothalamic integration: organization of the paraventricular and supraoptic nuclei. *Annu Rev Neurosci* **6**, 269–324.

Takeda K, Nakata T, Takesako T, Itoh H, Hirata M, Kawasaki S, Hayashi J, Oguro M, Sasaki S & Nakagawa M (1991). Sympathetic inhibition and attenuation of spontaneous hypertension by PVN lesions in rats. *Brain Res* **543**, 296–300.

Tanabe M, Gahwiler BH & Gerber U (1998). L-Type Ca^{2+} channels mediate the slow Ca^{2+}-dependent afterhyperpolarization current in rat CA3 pyramidal cells *in vitro*. *J Neurophysiol* **80**, 2268–2273.

Trabace L & Kendrick KM (2000). Nitric oxide can differentially modulate striatal neurotransmitter concentrations via soluble guanylate cyclase and peroxynitrite formation. *J Neurochem* **75**, 1664–1674.

Vaughan CW, Ingram SL, Connor MA & Christie MJ (1997). How opioids inhibit GABA-mediated neurotransmission. *Nature* **390**, 611–614.

de Vente J, Asan E, Gambaryan S, Markerink-van Ittersum M, Axer H, Gallatz K, Lohmann SM & Palkovits M (2001). Localization of cGMP-dependent protein kinase type II in rat brain. *Neuroscience* **108**, 27–49.

de Wardener HE (2001). The hypothalamus and hypertension. *Physiol Rev* **81**, 1599–1658.

Wood J & Garthwaite J (1994). Models of the diffusional spread of nitric oxide: implications for neural nitric oxide signalling and its pharmacological properties. *Neuropharmacology* **33**, 1235–1244.

Yang QZ & Hatton GI (1999). Nitric oxide via cGMP-dependent mechanisms increases dye coupling and excitability of rat supraoptic nucleus neurons. *J Neurosci* **19**, 4270–4279.

Yawo H (1999). Involvement of cGMP-dependent protein kinase in adrenergic potentiation of transmitter release from the calyx-type presynaptic terminal. *J Neurosci* **19**, 5293–5300.

Zagotta WN & Siegelbaum SA (1996). Structure and function of cyclic nucleotide-gated channels. *Annu Rev Neurosci* **19**, 235–263.

Zhang K, Li YF & Patel KP (2002). Reduced endogenous GABA-mediated inhibition in the PVN on renal nerve discharge in rats with heart failure. *Am J Physiol Regul Integr Comp Physiol* **282**, R1006–1015.

Zhang K & Patel KP (1998). Effect of nitric oxide within the paraventricular nucleus on renal sympathetic nerve discharge: role of GABA. *Am J Physiol* **275**, R728–734.

Acknowledgements

This study was supported by grants from the National Institutes of Health (NS45602, HL60026 and HL04199). D.-P. Li was supported by a postdoctoral fellowship from the American Heart Association, Pennsylvania–Delaware Affiliate. H.-L. Pan was a recipient of an Independent Scientist Award supported by the National Institutes of Health during the course of this study.